Araştırma Makalesi
Adıyaman Üniversitesi
Mühendislik Bilimleri Dergisi
23 (2024) 283-300

RSM-BASED MEASUREMENT OF CUTTING PERFORMANCE ON AL 7075 T6 AERO-STRUCTURAL ALLOY USING WEDM

Levent UĞUR[1], Kutay AYDIN[2*], Hakan KAZAN[3]

[1,2,3]Amasya Üniversitesi, Mühendislik Fakültesi, Makine Mühendisliği Bölümü, Amasya, 05100, Türkiye

Geliş Tarihi/Received Date: 04.04.2024 Kabul Tarihi/Accepted Date: 08.07.2024 DOI: 10.54365/adyumbd.1465339

ABSTRACT

Wire electrical discharge machining (WEDM) is a machining method commonly used in the aerospace, die making, automotive, and biomedical fields for machining complex and challenging shapes of conductive materials. WEDM is used in manufacturing to reduce power consumption while maintaining product quality. The current study used Response Surface Methodology(RSM) to investigate the relationship of WEDM parameters with surface roughness, kerf width, and power consumption for environmental concerns. Cutting parameters such as feed rate, pulse width, pulse space, and wire speed were chosen for experimental studies using 0.18 mm Guangming Molybdenum alloy wire. RSM was used to design experiments, analyze, and optimize WEDM independent parameters to minimize surface roughness, power consumption, and kerf width. The experiments yielded optimal cutting parameters. Analysis of variance (ANOVA) was used to determine important cutting parameters. Furthermore, a validation experiment was carried out to verify the performance of the optimum cutting parameters, which were found to be in good agreement with the experimental values. As a result, the most effective parameters for surface roughness, cutting power, and kerf width were discovered to be pulse width (67.96%), wire speed (54.96%), and pulse width (63.65%), respectively.

Keywords: *Wire cutting method, WEDM, Al 7075 T6, Surface roughness, Cutting power, Kerf width*

AL 7075 T6 HAVACILIK ALAŞIMININ WEDM İLE KESME PERFORMANSININ RSM TABANLI ARAŞTIRILMASI

ÖZET

Wire electrical discharge machining (WEDM), havacılık, kalıp ve kalıp yapımı, otomobil endüstrileri ve biyomedikal alanda karmaşık ve zorlu şekillerdeki iletken malzemelerin işlenmesi için yaygın olarak kullanılan bir işleme yöntemdir. WEDM Ürün kalitesinden ödün vermeden güç tüketimini en aza indirmek için üretim sektöründe önemli bir yere sahiptir. Bu doğrultuda, mevcut araştırma, WEDM parametrelerinin sürdürülebilirlik için yüzey pürüzlülüğü, kerf genişliği ve çevresel kaygı için güç tüketimi güç tüketimi ile ilişkisi Response Surface Methodology (RSM) ile araştırılmıştır. Deneysel araştırmalar için, 0,18 mm Guangming Molibden alaşım tel kullanılarak Feed rate, pulse width, pulse space ve wire speed gibi işleme parametreleri seçilmiştir. RSM, deneyleri tasarlamak ve yüzey pürüzlülüğünü, güç tüketimini ve kerf genişliğini en aza indirmek için WEDM'nin bağımsız parametrelerini analiz etmek ve optimize etmek için kullanılmıştır. Deneyler sonucunda optimum üretim parametreleri belirlendi. Varyans analizinden (ANOVA) önemli proses parametreleri belirlendi. Ayrıca, optimum proses parametrelerinin performansını doğrulamak için doğrulama deneyi yapılmış ve deneysel değerlerle iyi bir uyum içinde olduğu kaydedilmiştir. Sonuç olarak, yüzey pürüzlülüğü, kesme gücü ve kerf genişliği üzerindeki en etkin parametreler sırasıyla %67,96 oranla pulse width, 54,96 oranla wire speed, %63,65 oranla pulse width olduğu anlaşılmıştır.

Anahtar Kelimeler: *Tel erozyon yöntemi, WEDM, Al 7075 T6, Yüzey pürüzlülüğü, Kesme gücü, Kerf genişliği*

e-posta[1] : leventozge@gmail.com ORCID ID: https://orcid.org/0000-0003-3447-3191

[*] e-posta[2] : kutay.aydin@amasya.edu.tr ORCID ID: https://orcid.org/0000-0003-3614-4877 (Sorumlu Yazar)

e-posta[1] : hakan.kazan@amasya.edu.tr ORCID ID: https://orcid.org/0000-0001-7745-8974

Highlights

- RSM based Box-Behnken design using WEDM cutting for Al 7075 T6 alloy.
- Using molybdenum alloy as cutter wire in the WEDM process.
- Applying feed rate, pulse width, pulse space, and wire speed as cutting parameters.
- Effects of cutting parameters on surface roughness, cutting power, and kerf width.

Nomenclature

ANOVA	Analysis of variance	MRR	Material removal rate
CCD	Central Composite Design	P	Cutting power
CNC	Computerized numerical control	P_{cut}	Cutting power
df	Degree of freedom	ps	Pulse space
E_{arc}	Electric arc	pw	Pulse width
E_{conv}	Heat convection	Ra	Surface roughness
E_{rad}	Heat radiation	RHA	Rolled homogeneous armour
E_{total}	Toplam kesme enerjisi	RSM	Response surface methodology
f	Feed rate	V	Voltage
I	Current	w	Wire speed
ISO	International organization for standardization	WEDM	Wire electrical discharge machining
K	Kerf width		

1. Introduction

Aluminum and its alloys are indispensable engineering materials in various industrial applications due to their availability and superior machinability [1]. Among these alloys, the 7xxx series of aluminum alloys have garnered significant interest in the industry owing to their superior strength-to-weight ratio and lightness compared to other series such as Al-Si [2]. This lightweight characteristic has made them a prominent trend in modern aviation and automotive industries. Notably, Al 7075 T6 is extensively used in the construction of civil aviation aircraft, particularly in components such as the shell, nose, fuselage, and skeleton [3-5].

The traditional processing approach is insufficient for the needs of the aviation industry. Wire electric discharge machining (WEDM), which can produce parts with low dimensional deviation and high surface quality, is becoming more popular in the aviation industry. Furthermore, WEDM is becoming increasingly crucial in the manufacture of sensitive and complex geometries for a wide range of engineering applications [6-10].

WEDM is a non-traditional machining process commonly employed for electrically conductive materials that are difficult to cut, including Inconel, Hastelloy, graphite, steel, copper, aluminum, tungsten carbide, titanium, and metal matrix composites. This technique, which operates without direct contact, removes material by generating electrical spark discharges between the wire electrode and the workpiece. Its capability to cut electrically conductive materials regardless of their hardness or melting point provides a distinct advantage over traditional machining methods [11-13]. However, due to its primary use in processing low-conductivity and hard materials, the WEDM machining process incurs high energy consumption for melting and evaporation of electrodes [14]. Consequently, this directly impacts production costs, leading to an increase in the unit price per product. Therefore, in the context of sustainable machining operations, considerations such as energy consumption, surface finish, dimensional accuracy, and other machining performances are critical factors to be taken into account.

Bobbili et al. used the Buckingham Pi theorem to assess the effect of the inlet machining properties for WEDM of two different armor materials, such as aluminum alloy 7017 and RHA steel,

on material removal rate and surface roughness. The results showed that as the impact time value increased, so did the material removal rate (MRR) output response and surface roughness [15]. Grey Relational Analysis (GRA) was used by Kum et al. to optimize the kerf width and surface roughness during WEDM of a hard silicon carbide reinforced aluminum 6351 alloy composite. They claimed that the on-time pulse was the most effective in influencing the combined target, with 96.19 percent effectiveness [16]. Karabulut et al. conducted a study that considered the effect of processing parameters such as voltage, peak current, and wire tension on surface quality. Taguchi L27 full factorial array experimental design was used to optimize processing parameters, which were then followed by a mean effect plot and variance stub analysis. Three increasing parameter levels were used in the experiment. Following machining, it was discovered that peak current had a significant impact on surface roughness, wire tension, and spark gap [17]. Biswas et al investigated the Al 7075 WEDM processing parameters. For this alloy, a multi-objective genetic algorithm was used to optimize WEDM process parameters such as pulse width, pulse space, and wire tension. They recommended using pulse width (pw=0.2 μs), pulse space (ps=50 μs), and wire tension (Wt=1.1 kg) parameters for the best surface quality and machinability, respectively, as a result of the experiments and analyses [18]. In Shanthi et al. study, an analysis of variance (ANOVA) was performed and a mathematical model was developed to investigate the effect of WEDM's four input processing parameters on surface roughness. As a result of the experiments, it was discovered that the surface roughness increased with increasing pulse width and decreased with increasing pulse space and wire tension. It has been discovered that wire feeding has little effect on surface roughness [19].

Machining processes inherently prioritise important performance criteria such as energy efficiency, surface integrity and dimensional accuracy. Therefore, in this study, a comprehensive investigation is carried out for WEDM of Al 7075 T6, which is characterised by superior mechanical properties such as high tensile strength, ductility, toughness, favourable strength-to-weight ratio and resistance to high temperatures. Al 7075 T6 is known for being an indispensable material in many industrial sectors. However, the machining of this alloy faces significant challenges such as high cutting temperatures and rapid tool wear in conventional machining techniques. Due to these machining difficulties, this study involves the investigation of innovative cutting parameters tailored specifically for Al 7075 T6 through WEDM methodology. These parameters are expected not only to improve energy consumption, but also to improve surface finish and dimensional accuracy. This study aims to unlock the full potential of Al 7075 T6 by overcoming the limitations of conventional machining paradigms, and thus promote advances in machining efficiency and precision in various industrial sectors.

2. Experimental Work

The workpiece in the study was Al 7075 T6 aluminum alloy. Table 1 shows the chemical composition of the Al 7075 workpiece obtained from the manufacturer. Hightech DK-7732 CNC WEDM machine was used for the experiments. Guangming 0.18 mm The cutting wire was made of molybdenum alloy wire, and the insulating liquid was made of pure water and JR3A Ointment Coolant, 1/30-40 (kg/kg) (JR3A/pure water) dielectric emulsion. The wire is constantly used as a drum in looms that use molybdenum wire. The emulsion circulation pressure was kept constant at 1 bar. Figure 1 depicts the experimental setup, measurement, and analysis stages schematically.

Table 1. Chemical composition of Al 7075 T6 alloy

Alloy element	Al	Zn	Mg	Cu	Fe	Cr	Si	Mn	Zr	Ti
Wt. %	Base	5.1	2.1	1.2	0	0.18	0	0	0	0
		6.1	2.9	2	0.5	0.28	0.4	0.3	0.25	0.2

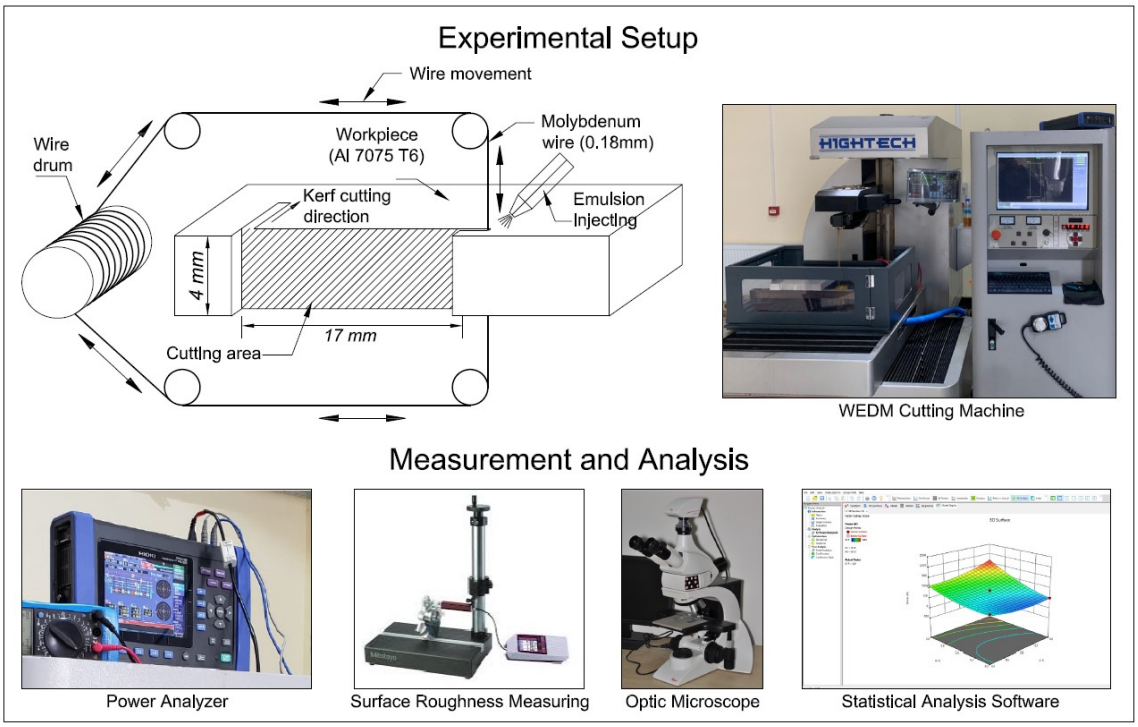

Figure 1. Experimental schema

Experiments were carried out using the Box-Behnken design of the Response Surface Methodology (RSM). Design-Expert® v12 software was used for statistical analysis. Cutting parameters such as feed rate, pulse width, pulse space, and wire speed were chosen as independent control factors. For each control factor, three levels are defined. The effects of cutting parameters on surface roughness, cutting power, and kerf width were investigated as a result of the experiments (Table 2). The cutting parameters are meticulously selected within the operational capacity of the wire erosion machine and informed by comprehensive review of pertinent literature [20]. A quadratic model was established in analysis of variance, and empirical equations were obtained through regression analysis. The Mitutoyo Surfest SJ-210 device was used to take the measurements. The measurements were taken in accordance with the ISO 4288 standard, with a cut-off length (λ_c) of 0.8mm and a traverse length (L_t) of 5.6mm. A Leica DM170M optical microscope was used to measure kerf width. Figure 2 depicts a schematic representation of kerf width measurement. Hioki Power Analyzer PW3198 was used to measure cutting power. Details of the equipment used in the experiment and measurement process are given in Table 3. The majority of the electrical energy used in WEDM cutting is used to generate the electric arc (E_{arc}) needed to melt the material between the wire and the workpiece. Furthermore, some of the energy is absorbed by the dielectric fluid through heat convection (E_{conv}). Heat radiation emits a very small amount of energy into the environment (E_{rad}). As a result, cutting energy is affected by the heat capacity, thermal conductivity, melting temperature, and other properties of the cutting wire, work material, and dielectric fluid. is determined by its physical and chemical properties [21]. Cutting energy can be expressed basically as in Equation 1.

$$E_{total} = E_{arc} + E_{conv} + E_{rad} \quad (1)$$

The measuring probes are connected between the wire and the workpiece to calculate the cutting force. As a consequence, the measured cutting power includes all components of the total cutting energy

(P). The breaking power was calculated by multiplying the power analyzer's average current (I) and average voltage (V) data during the cutting operation.

$$P_{cut} = I_{mean} \times V_{mean} \quad (2)$$

Table 2. Factors, levels, and responses

Factors	Symbol	Level 1 -1	Level 2 0	Level 3 1
Feed rate (mm/min)	f	2	2.5	3
Pulse width (µs)	pw	16	40	64
Pulse space (µs)	ps	88	284	480
Wire speed (m/s)	w	3	7.75	12.5
Responses	Ra, Surface roughness (µm) P, Cutting power (W) K, Kerf width (µm)			

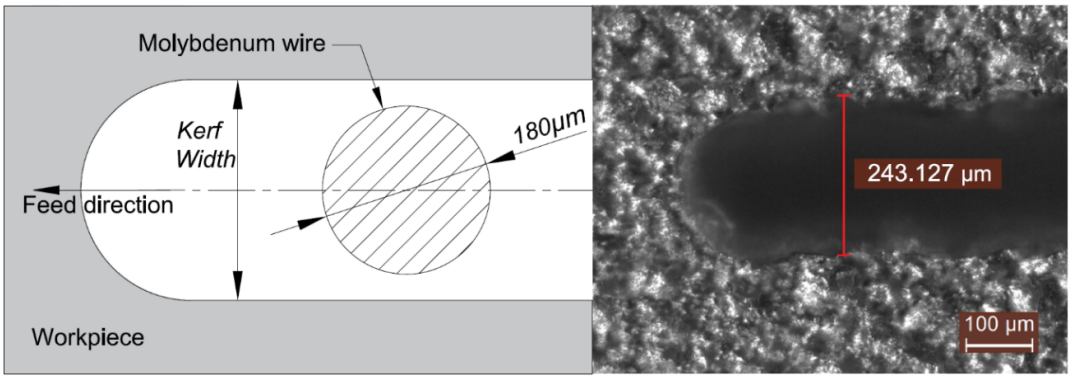

Figure 2. Top view of kerf width

Table 3. Test and measurement equipment and properties

Equipment	Properties
Hightech DK-7732 CNC WEDM machine	Wire: 0.18mm molybdenum alloy Coolant: JR3A Ointment Power: 2.3kW - 6kW
Hioki Power Analyzer PW3198	Standard: EN50160 Measuring time: 10s
Mitutoyo Surfest SJ-210 surface roughness measuring device	Standard: DIN EN ISO 3274 Resolution: 0.02 µm - 350 µm Probe: 2µm, 60º, 0.75 mN
Leica DM170M optical microscope	Illumination: 5000K led Magnification: 10x, 20x, 50x, 100x

3. Response Surface Methodology

Response surface methodology (RSM) is a set of mathematical and statistical techniques that can be used to model and analyze parameters of a process of significance to the researcher. The goal of this method is to optimize the parameters that it considers important [22, 23]. In classical approaches, only one variable is changed at a time in order to examine the effects of the process parameters on the

response functions during the experimental design. Unlike the traditional method, RSM reduces the number of experiments required and optimizes operating parameters in multivariate systems by taking into account the interactions between variables [24].

RSM was first introduced by Box and Wilson (1951) as a Central Composite Design (CCD)-based mathematical model suitable for the quadratic model and later developed for experimental design and data analysis [25]. The method includes a sequential process that employs statistical and mathematical techniques. The researcher investigates the type of appropriate approximation function, experimental design, optimum site selection, and transformation requirements for design variables using this method [26].

The RSM design process can be listed in three stages;

i. New experiment design (Sufficient and reliable measurement of responses),

ii. Developing the mathematical model with the best fit between the independent variables and the response and determining the optimum set of experimental parameters that give the upper and lower values of the response,

iii. Expressing the effects of process parameters with graphics [27].

The RSM method has two design types: Central Composite Design (CCD) and Box-Behnken Design (BBD) [28]. Among these, the modified central composite experimental design, known as the Box Behnken design, enables the calculation of the response function and estimation of the system performance at any experimental point in the examined range, with little work done [26]. The selection of the Box-Behnken design was made considering the purpose of the research, experimental conditions and analysis methods. This design is a response surface methodology experimental design commonly used to determine interactions between multiple variables and optimal conditions. Additionally, there are many examples showing that the Box-Behnken design has been widely used in the literature and has been successfully applied in similar research [29-31].

Design Expert 12 statistical software was used to create the experimental design. A total of 29 experiments were carried out in order to assess the attachments of the four major independent factors listed in Table 4 on Ra, P, and K. Because the material removal mechanism of WEDM has a very complex structure involving multiple physics phenomena, obtaining a statistical model based on the principle of electrical discharge generation is difficult. To establish the relationship between WEDM control variables and output responses such as Ra, P, and K, second-order polynomial regression models (quadratic model) were developed. The quadratic response model is represented by y in the equation, and the control parameters are symbolized by k [32].

$$y = \beta_0 + \sum_{j=1}^{k} \beta_j x_j + \sum_{j=1}^{k} \beta_{jj} x^2{}_j + \sum_{i}^{k-1} \sum_{j}^{k} \beta_{ij}\, x_i x_j + \varepsilon \tag{3}$$

In this equation; y response variable, β_0, β_1, β_2,.... β_k unknown regression parameters, x_i, x_j process (decision) variables ($i=1, 2, \ldots, k$) and ($j=1, 2, \ldots, k$), and ε error term [32].

4. Result and Discussion

Table 4 shows the experimental setup established in the RSM Box-Behnken design with the independent factors of feed rate, pulse width, pulse space, and wire speed. Table 4 displays the surface roughness, cutting power, and kerf width values obtained from the experiments for all cutting conditions.

Table 4. RSM matrix design and responses

Run	Factors				Responses		
	f (mm/min)	pw (µs)	ps (µs)	w (m/s)	Ra (µm)	P (W)	K (µm)
1	2.5	16	88	7.75	4.735	2.113	242.1
2	2.5	64	284	3	6.533	3.111	255.5
3	2	40	284	3	6.174	3.235	249.2
4	2	16	284	7.75	4.778	1.591	243.1
5	2.5	64	88	7.75	7.825	2.887	253.7
6	2.5	64	480	7.75	7.848	2.547	252.9
7	2.5	16	284	12.5	5.408	1.074	246.9
8	3	64	284	7.75	8.326	3.096	251.6
9	3	40	88	7.75	7.234	2.963	250.8
10	2.5	40	88	12.5	7.876	1.657	248.2
11	2.5	16	284	3	4.311	3.243	244.3
12	2.5	40	480	3	5.903	3.129	252.6
13	2.5	40	88	3	5.649	3.527	247.2
14	2.5	40	284	7.75	6.808	1.916	248.2
15	2.5	40	284	7.75	6.718	1.997	248.7
16	2	40	480	7.75	7.254	2.129	250.9
17	2.5	40	284	7.75	6.714	1.783	250.6
18	3	16	284	7.75	4.897	2.693	247.6
19	2.5	40	284	7.75	6.719	1.839	248.9
20	2.5	40	480	12.5	7.313	2.063	249.1
21	2	40	284	12.5	7.646	1.188	247.2
22	3	40	480	7.75	7.036	3.246	250.6
23	2.5	64	284	12.5	9.134	1.984	250.5
24	2	40	88	7.75	7.283	2.115	246.5
25	2.5	40	284	7.75	6.720	2.089	250.4
26	3	40	284	12.5	8.012	2.548	249.8
27	2.5	16	480	7.75	4.945	2.497	249.2
28	2	64	284	7.75	8.745	2.467	253.5
29	3	40	284	3	5.366	3.559	249.3

4.1. Analysis of surface roughness

Surface roughness is great of importance in terms of metalworking and tribology since it defines the material properties such as friction, corrosion, fatigue, lubrication, etc [33]. Also, it is an important factor in determining the production quality [34]. As a result, the values of surface roughness were investigated in this study. Figure 3 depicts the effects of changing cutting conditions on surface roughness. The graphs were made in the shape of a surface graph, showing the interaction of two independent factors as well as their effects on surface roughness (Figure 3). Examining the graphics reveals a correlation between rising surface roughness values when the pulse width and wire speed are increased. The electron flow from the wire to the workpiece increases as the pulse width and wire speed are increased. The size of the micro-craters on the workpiece grows as the electron bombardment

increases. This situation is thought to increase the surface roughness values [12, 35, 36]. Although increasing the pulse space slightly increases the surface roughness values, it has no significant effect. The change in feed rate had no effect on surface roughness as well. Surface roughness is expected to decrease in wedm machining operations due to an increase in pulse space and a decrease in feed rate as the insulating cutting fluid moves the chips away from the cutting zone [22, 37]. However, it is clear that this situation does not apply to the Al 7075 T6 alloy. Aluminum alloys have low melting points but high heat transfer coefficients. It is believed that the material, which melts rapidly when bombarded with electrons, solidifies quickly again before it can move away from the cutting zone during the waiting period [38]. Therefore, it can be interpreted that the pulse space and feed rate parameters do not have a significant effect on the surface roughness due to the presence of residual debris and craters on the cutting surface during the waiting period without electron bombardment.

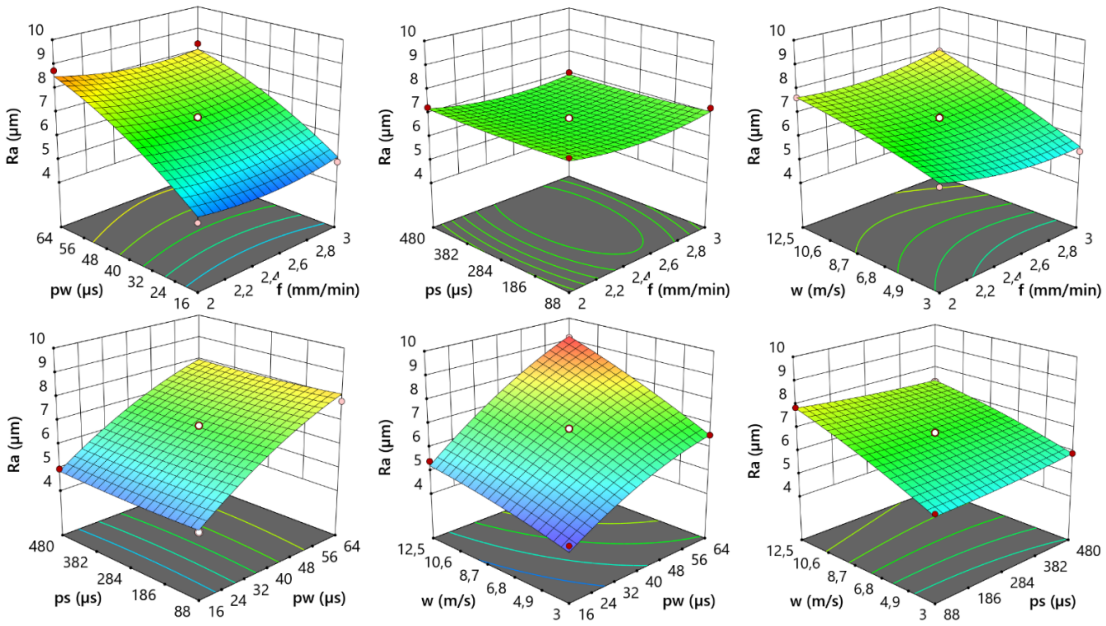

Figure 3. Effect of cutting parameters on surface roughness

Variance and regression data analyses were carried out with a 95% confidence level, assuming that the surface roughness results vary depending on the feed rate, pulse width, pulse space, and wire speed parameters chosen as independent control factors. Table 5 shows the results of the analysis of variance and the percentage contribution ratio (C-value). As the results shows that some P values exceeded 5% ($P<0.05$). However, the P values for the model and effective parameters ($P<0.0001$) are quite low. In addition, the F values of the model and the active parameters appear to be 4.196 greater than the critical F value ($F_{.05,1,28}$). Thus, the selection of control factors and levels can be considered to be statistically significant [39]. In terms of surface roughness, the most effective cutting parameters were found to be pulse width and wire speed, with C-value ratios of 67.96% and 23.84%, respectively. When the coefficients of determination (R^2) are examined, the surface roughness model is found to be 98.7% compatible with the experimental results (Table 5). Equation 4 depicts the empirical mathematical model derived from regression analysis. Figure 4 depicts measurement-estimate values and residual plot graphs for surface roughness. The graphs show that the measured and estimated surface roughness values are compatible and at an acceptable level. The solid line indicates that the level of error is normal [40, 41]. From the residual plot graph, it can be interpreted that the residues are at the normal level due to the accumulation along the straight line.

Table 5. ANOVA table for surface roughness

Source	Sum of Squares	df	Mean Square	F-value	p-value	C-value
Model	45.2516	14	3.2323	75.88	<0.0001	98.70
f	0.0848	1	0.0848	1.99	0.1800	0.19
pw	31.1600	1	31.1600	731.50	<0.0001	67.96
ps	0.0077	1	0.0077	0.18	0.6782	0.02
w	10.9309	1	10.9309	256.61	<0.0001	23.84
f.pw	0.0724	1	0.0724	1.70	0.2135	0.16
f.ps	0.0071	1	0.0071	0.17	0.6884	0.02
f.w	0.3446	1	0.3446	8.09	0.0130	0.75
pw.ps	0.0087	1	0.0087	0.21	0.6575	0.02
pw.w	0.5655	1	0.5655	13.28	0.0027	1.23
ps.w	0.1669	1	0.1669	3.92	0.0678	0.36
f^2	0.5826	1	0.5826	13.68	0.0024	1.27
pw^2	0.8340	1	0.8340	19.58	0.0006	1.82
ps^2	0.0304	1	0.0304	0.71	0.4126	0.07
w^2	0.1072	1	0.1072	2.52	0.1349	0.23
Residual	0.5964	14	0.0426			1.30
Lack of Fit	0.5898	10	0.0590	36.09	0.0018	1.29
Pure Error	0.0065	4	0.0016			0.01
Cor Total	45.8480	28				100.00
Fit Statistics						
Std. Dev.	0.2064		R^2	0.9870		
Mean	6.6866		Adjusted R^2	0.9740		
C.V. %	3.0867		Predicted R^2	0.9257		
			Adeq Precision	34.5716		

$$\boldsymbol{Ra} = 10.64149 - (6.54880 \times f) + (0.12223 \times pw) + (2.04 \times 10^{-3} \times ps) - (0.08932 \times w) - (0.01121 \times f \times pw) - (4.31 \times 10^{-4} \times f \times ps) + (0.12358 \times f \times w) - (9.94 \times 10^{-6} \times pw \times ps) + (3.30 \times 10^{-3} \times pw \times w) - (2.19 \times 10^{-4} \times ps \times w) + (1.19873 \times f^2) - (6.23 \times 10^{-4} \times pw^2) + (1.78 \times 10^{-6} \times ps^2) - (5.70 \times 10^{-3} \times w^2) \quad (4)$$

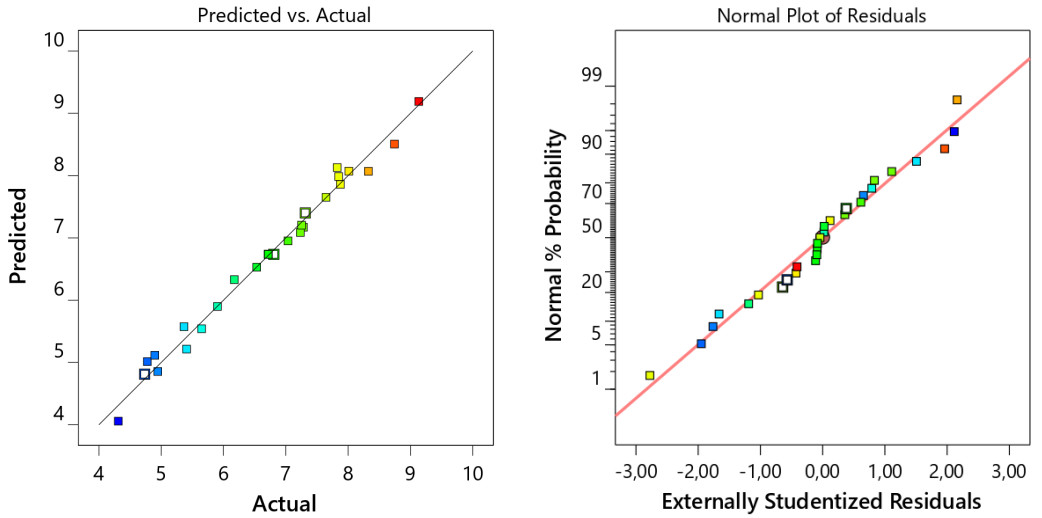

Figure 4. RSM versus experimental predicted values and residuals plot for surface roughness (Ra)

The images needed for topographic analysis are obtained with the Leica DM170M optical microscope. High-resolution images of the workpiece are obtained in the magnification 10x. The acquired images are visualized stacking in Z direction in the Matlab® program for step height, surface/line smoothness, and area/volume measurement. The topographic process is carried out on a specific area of 800x800µm. The results of surface topography of the experiments with the lowest surface roughness (Run no. 11) and the highest surface roughness (Run no. 23) obtained from the WEDM are shown in Figure 5. When examining the topographic surface of experiment 23, the increase in pw and w values appears to be coarse morphology on the WEDM cutting surface. Serious thermal damage to the machined component that produces a high energy discharge pulse. In contrast, when examining the topographic surface of experiment 11, minimal thermal damage to the WEDM cut-off surface of the Al 7075 T6 aluminum components produces a low density and low energy discharge pulse.

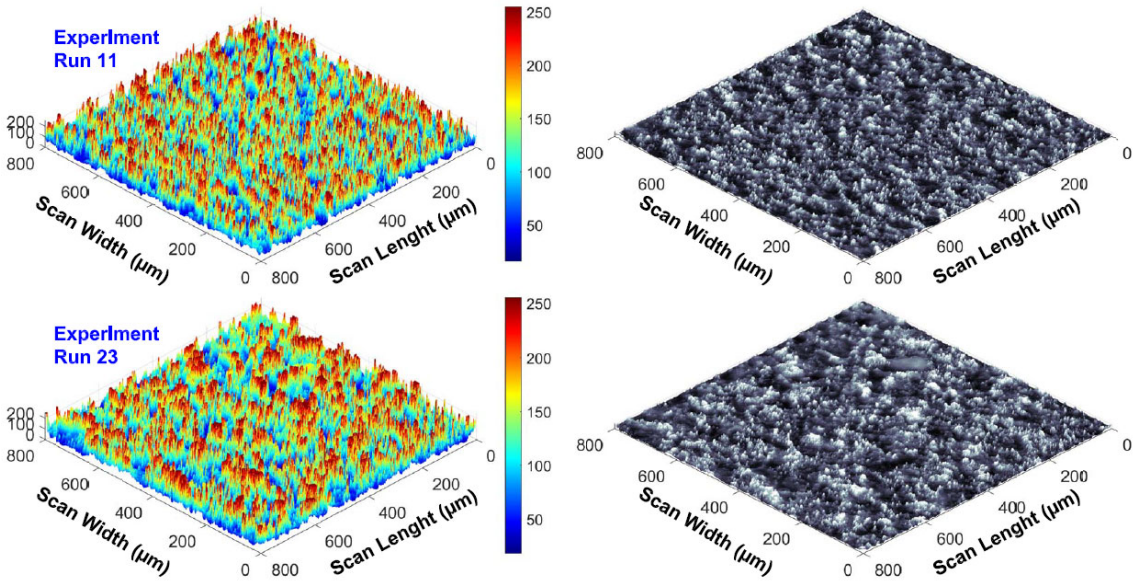

Figure 5. Cutting surface topographies of maximum (run 23) and minimum (run 11) surface roughness

4.2. Analysis of cutting power

Cutting power is a critical factor in determining production costs in the manufacturing sector, and therefore, the study also evaluated the cutting power output. Figure 6 illustrates the effects of changing cutting conditions on cutting power. In WEDM processes, due to the low feed rate and the use of coolant, there are chips adhering to the cutting surface that need to be remelted. As the wire speed increases, these chips are removed from the cutting zone more rapidly since wire movement occurs in the direction of gravity, aiding the coolant in removing chips from the cutting zone. The graph demonstrates a significant decrease in cutting power values when wire speed increases and feed rate decreases. This reduces the amount of chips that melt and resolidify. Consequently, as the amount of chips adhering to and needing to be remelted on the cutting surface decreases, the cutting power decreases. A reduction in feed rate has a similar effect; when the feed rate is decreased, the cleaning time of the cutting fluid increases, allowing for more effective chip removal. This also explains the decrease in cutting power. However, changes in pulse width and pulse space appear to have no effect on cutting power.

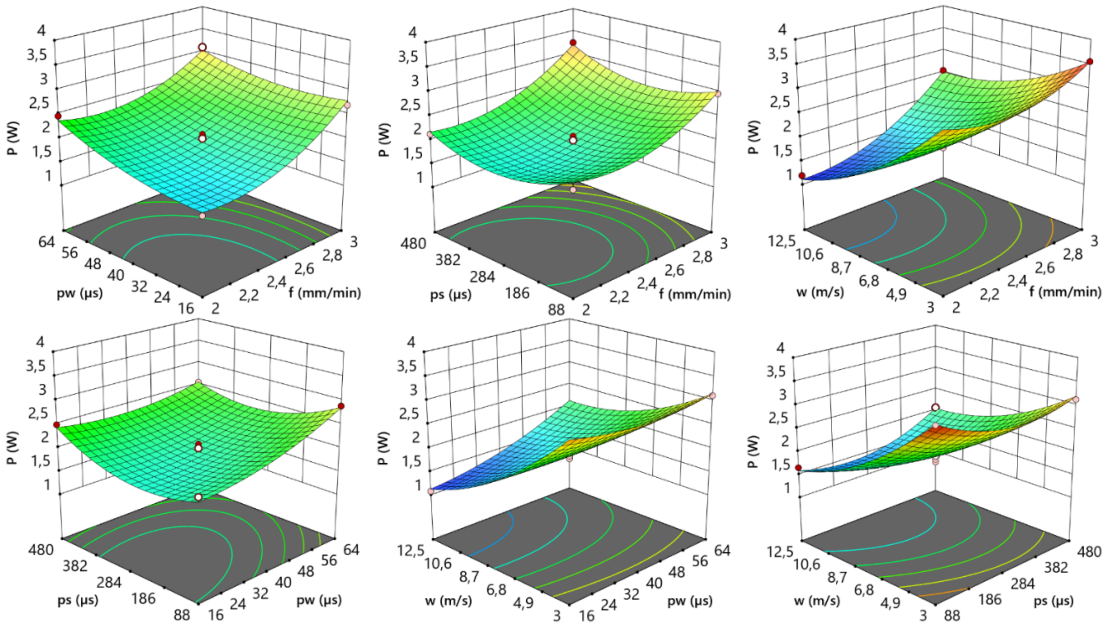

Figure 6. Effect of cutting parameters on cutting power

Variance and regression data analyzes were performed with the assumption that the cutting power findings vary according to the independent control factors and with a 95% confidence level. The results of analysis of variance and % contribution ratio (C-value) are given in Table 6. Some P values were found to be greater than 5% ($P<0.05$) according to the results. The P values of the model and the effective parameters ($P<0.0001$), on the other hand, are quite low. Furthermore, the model and active parameter F values appear to be 4.196 greater than the critical F value ($F_{.05,1,28}$). As a result, the choice of control factors and levels can be considered statistically significant [39]. Wire speed and feed rate were found to be the most efficient cutting parameters in terms of cutting power, with C-values of 54.96% and 18.43%, respectively. The coefficients of determination (R^2) show that the cutting power model is 98.7% compatible with the experimental results (Table 6). Equation 5 depicts the empirical mathematical model derived from regression analysis. Figure 7 depicts measurement-estimate values and residual plot graphs for cutting power. The graphs show that the measured and estimated cutting power values are compatible and at an acceptable level. The solid line indicates that the level of error is normal [40, 41]. The residual plot graph indicates that the residues are at normal levels due to accumulation along the straight line.

Table 6. ANOVA table for cutting power

Source	Sum of Squares	df	Mean Square	F-value	p-value	C-value
Model	12.9158	14	0.9226	75.99	<0.0001	98.70
f	2.4120	1	2.4120	198.67	0.0000	18.43
pw	0.6917	1	0.6917	56.97	0.0000	5.29
ps	0.0102	1	0.0102	0.84	0.3760	0.08
w	7.1920	1	7.1920	592.37	<0.0001	54.96
f.pw	0.0559	1	0.0559	4.61	0.0498	0.43
f.ps	0.0181	1	0.0181	1.49	0.2424	0.14
f.w	0.2683	1	0.2683	22.10	0.0003	2.05
pw.ps	0.1310	1	0.1310	10.79	0.0054	1.00
pw.w	0.2714	1	0.2714	22.36	0.0003	2.07

ps.w	0.1616	1	0.1616	13.31	0.0026	1.23
f^2	0.8583	1	0.8583	70.70	<0.0001	6.56
pw^2	0.1939	1	0.1939	15.97	0.0013	1.48
ps^2	0.8839	1	0.8839	72.80	<0.0001	6.75
w^2	0.5829	1	0.5829	48.01	<0.0001	4.45
Residual	0.1700	14	0.0121			1.30
Lack of Fit	0.1103	10	0.0110	0.74	0.6834	0.84
Pure Error	0.0597	4	0.0149			0.46
Cor Total	13.0858	28				100.00
Fit Statistics						
Std. Dev.	0.1102		R^2	0.9870		
Mean	2.4237		Adjusted R^2	0.9740		
C.V. %	4.5463		Predicted R^2	0.9443		
			Adeq Precision	30.8535		

$$\boldsymbol{P} = 14.01257 - (7.02455 \times f) + (0.00384 \times pw) - (0.00716 \times ps) - (0.79427 \times w) - (0.00985 \times f \times pw) + (6.86 \times 10^{-4} \times f \times ps) + (0.10905 \times f \times w) - (3.85 \times 10^{-5} \times pw \times ps) + (0.00229 \times pw \times w) + (2.16 \times 10^{-4} \times ps \times w) + (1.45507 \times f) + (3.00 \times 10^{-4} \times pw) + (9.61 \times 10^{-6} \times ps) + (0.01329 \times w) \quad (5)$$

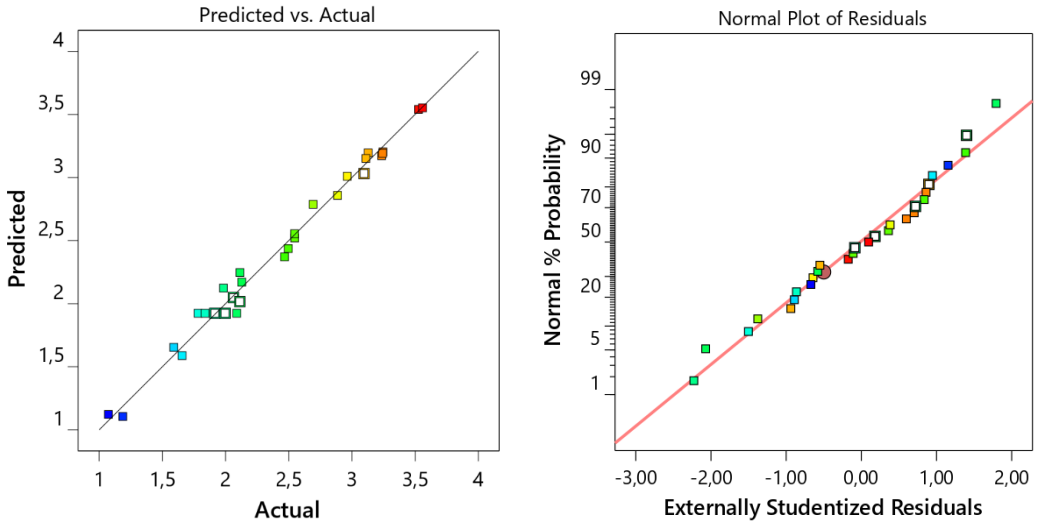

Figure 7. RSM versus experimental predicted values and residuals plot for cutting power (P)

4.3. Analysis of kerf width

As a critical parameter in machining processes, kerf width is crucial for post-processing dimensional accuracy and final product quality. Therefore, an extensive research was conducted to understand the kerf width values. The findings presented in Figure 8 clearly show the effect of various cutting conditions on kerf width. Detailed analysis of the graph reveals that there is a significant increase in kerf width values with increasing pulse width. This increase is related to the fact that the pulse width increases the electron bombardment applied to the workpiece. Increased bombardment leads to more intense melting and larger chip formation in the cutting zone, resulting in an increase in kerf width [42-44]. This emphasizes that kerf width plays a critical role in the machining process and is a parameter that needs to be carefully monitored. The study also revealed a slight increase in kerf width with increasing pulse space and feed rate [43]. This is because pulse width and feed rate increase the kerf

width by supporting each other, while pulse space and feed rate parameters suppress the effect of each other. Pulse space and pulse width parameters show opposite effects in terms of kerf width [36]. However, at low pulse width values, the effect of wire speed on kerf width is uncertain. On the contrary, at high pulse width values, kerf width decreases as the wire speed increases. The reason for this is thought to be the rapid cleaning of the cutting zone from chip with the increase in wire speed during cutting at high pulse width values. This finding underlines the complex interaction between various cutting parameters and their cumulative effect on kerf width.

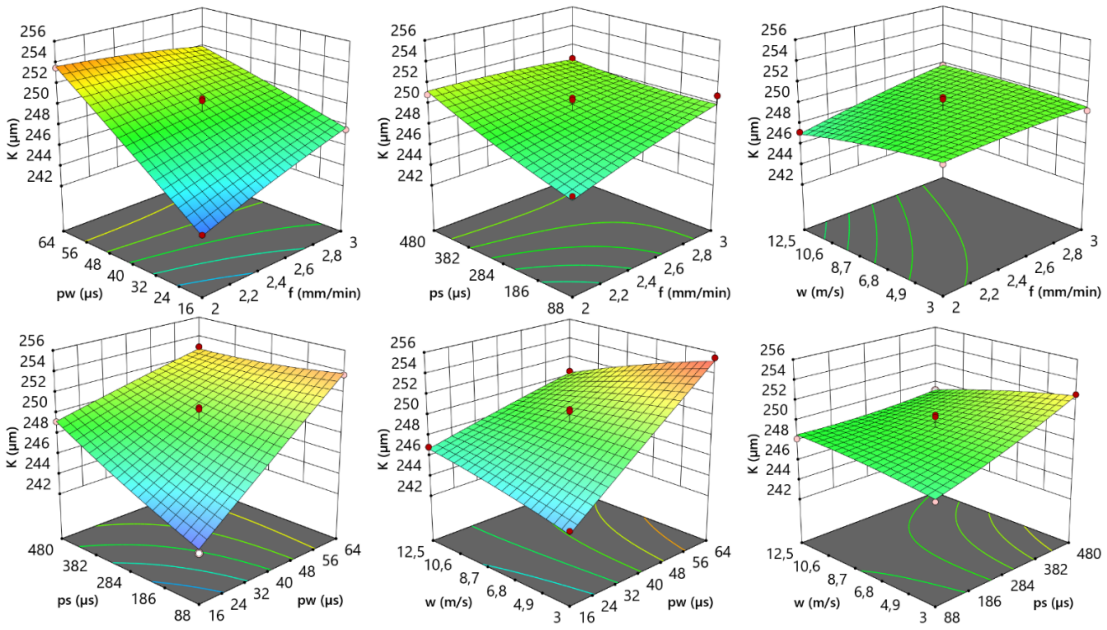

Figure 8. Effect of cutting parameters on kerf width

Table 7 shows the results of the analysis of variance in terms of kerf width and % contribution ratio (C-value). The results demonstrated that some P values exceeded 5% ($P<0.05$). However, the P values for the model and effective parameters ($P<0.0001$) are quite low. Furthermore, the model and active parameter F values appear to be 4.196 greater than the critical F value ($F_{.05,1,28}$). As a result, the choice of control factors and levels can be considered statistically significant [39]. In terms of kerf width, the most effective cutting parameters were found to be pulse width and pulse space, with C-value ratios of 63.65% and 9.07%, respectively. Examining the coefficients of determination (R^2) reveals that the kerf width model agrees with the experimental findings at a rate of 97.46%. (Table 7). Equation 6 represents the empirical mathematical model derived from regression analysis. Figure 9 depicts measurement-estimate values and residual plot graphs for kerf width. The graphs show that the measured and estimated kerf width values are compatible and at an acceptable level. The solid line indicates that the level of error is normal [40, 41]. From the residual plot graph, it can be understood that the residues are at the normal level due to the accumulation along the straight line.

Table 7. ANOVA table for kerf width

Source	Sum of Squares	df	Mean Square	F-value	p-value	C-value
Model	252.6498	14	18.0464	38.29	<0.0001	97.46
f	7.2075	1	7.2075	15.29	0.0016	2.78
pw	165.0208	1	165.0208	350.16	<0.0001	63.65
ps	23.5200	1	23.5200	49.91	<0.0001	9.07
w	3.4133	1	3.4133	7.24	0.0176	1.32
f.pw	10.2400	1	10.2400	21.73	0.0004	3.95
f.ps	5.2900	1	5.2900	11.22	0.0048	2.04
f.w	1.5625	1	1.5625	3.32	0.0901	0.60
pw.ps	15.6025	1	15.6025	33.11	<0.0001	6.02
pw.w	14.4400	1	14.4400	30.64	<0.0001	5.57
ps.w	5.0625	1	5.0625	10.74	0.0055	1.95
f^2	0.2102	1	0.2102	0.45	0.5151	0.08
pw^2	0.0415	1	0.0415	0.09	0.7710	0.02
ps^2	0.5177	1	0.5177	1.10	0.3124	0.20
w^2	0.3069	1	0.3069	0.65	0.4332	0.12
Residual	6.5978	14	0.4713			2.54
Lack of Fit	1.9858	10	0.1986	0.17	0.9889	0.77
Pure Error	4.6120	4	1.1530			1.78
Cor Total	259.2476	28				100.00
Fit Statistics						
Std. Dev.	0.6865		R^2	0.9746		
Mean	249.2793		Adjusted R^2	0.9491		
C.V. %	0.2754		Predicted R^2	0.9281		
			Adeq Precision	25.7736		

$$\boldsymbol{K} = 204.27580 + (11.77651 \times f) + (0.74736 \times pw) + (0.05846 \times ps) + (0.38909 \times w) - (0.133 \times f \times pw) - (0.01174 \times f \times ps) + (0.26316 \times f \times w) - (4.20 \times 10^{-4} \times pw \times ps) - (0.01667 \times pw \times w) - (1.21 \times 10^{-3} \times ps \times w) - (0.72 \times f^2) - (1.39 \times 10^{-4} \times pw^2) + (7.35 \times 10^{-6} \times ps^2) - (0.00964 \times w^2) \quad (6)$$

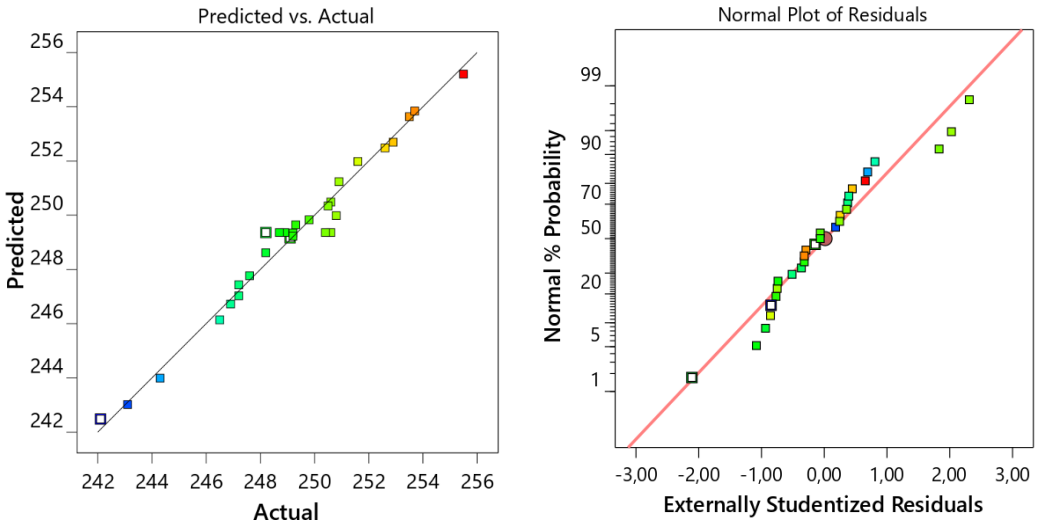

Figure 9. RSM versus experimental predicted values and residuals plot for kerf width (K)

4.4. Confirmation experiments

Three prediction tests were carried out in the study for the verification tests, in machining conditions not listed in Table 4, where surface roughness, cutting power, and kerf width outputs were minimal. Table 8 shows the percentage error rates between the measured surface roughness, cutting power, and kerf width values and the RSM results. The error rates were calculated using the equation in Equation 7.

$$\boldsymbol{Error}\ \% = [(measured\ result - predicted\ result)/measured\ result] \times 100 \quad (7)$$

Table 8 shows that there is more than 98% agreement between the measured values and the predicted values. It was understood that the error rates between the measured and predicted data were very low, and the prediction performance of the statistical model was at a satisfactory level as in similar studies [6, 29].

Table 8. Optimization of response parameters

Run	Optimize value of factor				Response	Measured value	Predicted value	Error %
	f (mm/min)	pw (µs)	ps (µs)	w (m/s)				
1	2.27	16	168.59	7.33	Ra (µm)	*4.792**	*4.754**	0.79
					P (W)	1.795	1.812	0.95
					K (µm)	241.3	242.1	0.33
2	2.12	16	176.16	10.09	Ra (µm)	5.193	5.091	1.96
					P (W)	*1.067**	*1.074**	0.66
					K (µm)	243.5	242.1	0.57
3	2.12	16	176.12	10.09	Ra (µm)	5.101	5.091	0.20
					P (W)	1.086	1.074	1.10
					K (µm)	*239.2**	*241.1**	0.79

5. Conclusion

In this study, the effects of different machining conditions on surface roughness, cutting power and kerf width were investigated by machining Al 7075 T6 aluminum alloy through WEDM. In this context, experimental study and statistical analyzes were carried out in the RSM Box-Behnken design by selecting the feed rate, pulse width, pulse space and wire speed parameters. The results are summarized as follows:

- Surface roughness values increase with increasing pulse width and wire speed. No significant effect of other cutting parameters was observed.
- Cutting power decreases significantly with increase in wire speed and decrease in feed rate. Other factors have little influence.
- Kerf width amounts increase significantly with increasing pulse width. A slight increase was observed with the increase in pulse space and feed rate. No significant effect of the wire speed factor was observed.

- In terms of variance analysis; The most effective parameters on surface roughness, cutting power and kerf width were found to be pulse width with 67.96%, wire speed with 54.96% and pulse width with 63.65%, respectively.
- In terms of regression analysis; The coefficients of determination (R^2) of the models were obtained as 98.7%, 98.7% and 97.46 for surface roughness, cutting power and kerf width, respectively. These ratios showed that the measurements and the estimation were in agreement.

Competing Interests: Authors declare there is no conflict of interest.

Funding Information: There were no public or private sources of funding.

Author Contribution: The authors confirms responsibility for the following: study conception and design, data collection, analysis and interpretation of results, and manuscript preparation.

Data Availability Statement: The data generated and/or analyzed during the current study are not publicly available, but data may be provided by the corresponding author upon reasonable request.

Conflict Of Interest

The authors declare that they have no conflict of interest.

References

[1] Feng, L, Che, Y, Liu, Y, Qiang, X, and Wang, Y. Fabrication of superhydrophobic aluminium alloy surface with excellent corrosion resistance by a facile and environment-friendly method. Applied Surface Science. 2013;283:367-374.
[2] Zuo, M, Sokoluk, M, Cao, C, Yuan, J, Zheng, S, and Li, X. Microstructure control and performance evolution of aluminum alloy 7075 by nano-treating. Scientific reports. 2019;9(1):1-11.
[3] Attahu, CY, An, L, Li, Z, and Gao, G. Influence of shim layers on progressive failure of a composite component in composite-aluminum bolted joint in aerospace structural assembly. Transactions of Nanjing University of Aeronautics and Astronautics. 2018;35(1):188-202.
[4] Yang, Y, Li, M, and Li, K. Comparison and analysis of main effect elements of machining distortion for aluminum alloy and titanium alloy aircraft monolithic component. The International Journal of Advanced Manufacturing Technology. 2014;70(9):1803-1811.
[5] Singh, AK, Singhal, D, and Kumar, R. Machining of aluminum 7075 alloy using EDM process: An ANN validation. Materials Today: Proceedings. 2020;26:2839-2844.
[6] Sharma, P, Chakradhar, D, and Narendranath, S. Measurement of WEDM performance characteristics of aero-engine alloy using RSM-based TLBO algorithm. Measurement. 2021;179:109483.
[7] Dewan, P, Kundu, P, and Phipon, R. Powder mixed electric discharge machining–A review. AIP Conference Proceedings. AIP Publishing, 2020.
[8] Dewan, PR and Kundu, PK. On Titanium Powder Mixed Electric Discharge Machining of Nimonic C-263. Journal of The Institution of Engineers (India): Series D. 2022:1-8.
[9] Dewan, PR and Kundu, PK. Optimizing process parameters for EDM of nimonic C-263 under green dielectric. Sādhanā. 2023;48(4):230.
[10] Goyal, A and Ur Rahman, H. Experimental studies on Wire EDM for surface roughness and kerf width for shape memory alloy. Sādhanā. 2021;46(3):160.
[11] Das, S and Joshi, SN. Measurement and analysis of molybdenum wire erosion and deformation during wire electric discharge machining of Ti-6Al-4V alloy. Measurement. 2021;179:109440.

[12] Kanlayasiri, K and Boonmung, S. Effects of wire-EDM machining variables on surface roughness of newly developed DC 53 die steel: Design of experiments and regression model. Journal of materials processing technology. 2007;192:459-464.
[13] Zheng, J, Lai, X, Chen, A, and Zheng, W. Energy modeling and minimizing energy consumption control strategy of wire electrical discharge machining (WEDM) through electrical parameters. The International Journal of Advanced Manufacturing Technology. 2019;103(9):4341-4353.
[14] Shastri, RK and Mohanty, CP. Sustainable electrical discharge machining of Nimonic C263 superalloy. Arabian Journal for Science and Engineering. 2021;46(8):7273-7293.
[15] Bobbili, R, Madhu, V, and Gogia, A. Modelling and analysis of material removal rate and surface roughness in wire-cut EDM of armour materials. Engineering Science and Technology, an International Journal. 2015;18(4):664-668.
[16] Kumar, SS, Uthayakumar, M, Kumaran, ST, Parameswaran, P, Mohandas, E, Kempulraj, G, Babu, BR, and Natarajan, S. Parametric optimization of wire electrical discharge machining on aluminium based composites through grey relational analysis. Journal of Manufacturing Processes. 2015;20:33-39.
[17] Karabulut, Ş, Kökçan, R, Bilgin, M, and Özdemir, A. Study on the Wire Electrical Discharge Machining of AA 7075 Aluminum Alloy. 2018 9th International Conference on Mechanical and Aerospace Engineering (ICMAE). IEEE, 2018.
[18] Biswas, MS, Mandal, K, and Sarkar, S. MOGA approach in WEDM of advanced aluminium alloy. Materials Today: Proceedings. 2020;26:887-890.
[19] Jayachandran, S, Raman, M, and Ramasamy, T. Experimental investigation for the optimization of the WEDM process parameters to obtain the minimum surface roughness of the Al 7075 aluminium alloy employed with a zinc-coated wire using RSM and GA. Materiali in Tehnologije. 2019;53(3):349-356.
[20] Aydın, K, Uğur, L, Güvercin, S, and Gül, F. Investigation of the machining performance of ferritic ductile cast Iron in WEDM using response surface methodology. Sigma Journal of Engineering and Natural Sciences. 2022;40(1):95-107.
[21] Zhang, Z, Yu, H, Zhang, Y, Yang, K, Li, W, Chen, Z, and Zhang, G. Analysis and optimization of process energy consumption and environmental impact in electrical discharge machining of titanium superalloys. Journal of Cleaner Production. 2018;198:833-846.
[22] Sharma, N, Khanna, R, and Gupta, R. Multi quality characteristics of WEDM process parameters with RSM. Procedia Engineering. 2013;64:710-719.
[23] Anderson-Cook, CM, Borror, CM, and Montgomery, DC. Response surface design evaluation and comparison. Journal of Statistical Planning and Inference. 2009;139(2):629-641.
[24] Shandilya, P, Jain, P, and Jain, N. RSM and ANN modeling approaches for predicting average cutting speed during WEDM of SiCp/6061 Al MMC. Procedia Engineering. 2013;64:767-774.
[25] Box, GE and Hunter, JS. Multi-factor experimental designs for exploring response surfaces. The Annals of Mathematical Statistics. 1957:195-241.
[26] Murat, D, Ensarioğlu, C, Gürsakal, N, Oral, A, and Çakır, MC. Evaluation of tool wear for hard turning operations through response surface methodology. 2018.
[27] Gunaraj, V and Murugan, N. Application of response surface methodology for predicting weld bead quality in submerged arc welding of pipes. Journal of materials processing technology. 1999;88(1-3):266-275.
[28] Montgomery, DC. Design and analysis of experiments: John wiley & sons; 2017.
[29] Raj, A, Misra, J, Khanduja, D, Saxena, K, and Malik, V. Design, modeling and parametric optimization of WEDM of Inconel 690 using RSM-GRA approach. International Journal on Interactive Design and Manufacturing (IJIDeM). 2022:1-11.
[30] Ishfaq, K, Anwar, S, Ali, MA, Raza, MH, Farooq, MU, Ahmad, S, Pruncu, CI, Saleh, M, and Salah, B. Optimization of WEDM for precise machining of novel developed Al6061-7.5% SiC squeeze-casted composite. The International Journal of Advanced Manufacturing Technology. 2020;111:2031-2049.
[31] Dzionk, S and Siemiątkowski, MS. Studying the effect of working conditions on WEDM machining performance of super alloy Inconel 617. Machines. 2020;8(3):54.

[32] Anderson, MJ and Whitcomb, PJ. RSM simplified: optimizing processes using response surface methods for design of experiments: Productivity press; 2016.
[33] Altın Karataş, M. Inconel 718'in tel erozyon ile işlenmesinde yüzey pürüzlülüğünün Taguchi tabanlı gri ilişkisel analiz yöntemi ile çok kriterli optimizasyonu. Pamukkale Üniversitesi Mühendislik Bilimleri Dergisi. 2022;28(4):516-532.
[34] Dobes, J, Leal, JES, Profeta, J, de Sousa, MM, Neto, FPL, Piratelli-Filho, A, and Arencibia, RV. Effect of mechanical vibration on Ra, Rq, Rz, and Rt roughness parameters. The International Journal of Advanced Manufacturing Technology. 2017;92(1):393-406.
[35] Azam, M, Jahanzaib, M, Abbasi, JA, and Wasim, A. Modeling of cutting speed (CS) for HSLA steel in wire electrical discharge machining (WEDM) using moly wire. Journal of the Chinese Institute of Engineers. 2016;39(7):802-808.
[36] Gajjar, DH and Desai, JV. Optimization of MRR, Surface Roughness and KERF Width in wire EDM Using Molybdenum Wire. International Journal for Research in Education. 2015;4(2).
[37] Soota, T and Rajput, S. Optimization and measurement of kerf width and surface roughness of AISI 316L. Forces in Mechanics. 2022;6:100071.
[38] Çaydaş, U and Hasçalık, A. Tel Erozyon Yönteminde İşleme Parametrelerinin Alüminyum Alaşımının Yüzey Yapısına Etkisi. Politeknik Dergisi. 2004;7(1):31-36.
[39] Bolar, G, Das, A, and Joshi, SN. Measurement and analysis of cutting force and product surface quality during end-milling of thin-wall components. Measurement. 2018;121:190-204.
[40] Kaçal, A and Yıldırım, F. PMD23 Çeliğinin Tornalanmasında CBN Kesici Uçların Kesme Performansının Yüzey Pürüzlülüğü ve Takım Aşınması Üzerindeki Etkilerinin Belirlenmesi. Gazi Üniversitesi Mühendislik Mimarlık Fakültesi Dergisi. 2016;31(1).
[41] Asiltürk, I, Neşeli, S, and Ince, MA. Optimisation of parameters affecting surface roughness of Co28Cr6Mo medical material during CNC lathe machining by using the Taguchi and RSM methods. Measurement. 2016;78:120-128.
[42] Goswami, A and Kumar, J. Optimization in wire-cut EDM of Nimonic-80A using Taguchi's approach and utility concept. Engineering Science and Technology, an International Journal. 2014;17(4):236-246.
[43] Tosun, N, Cogun, C, and Tosun, G. A study on kerf and material removal rate in wire electrical discharge machining based on Taguchi method. Journal of materials processing technology. 2004;152(3):316-322.
[44] Koklu, U. Optimization of Kerf and Surface Roughness of AL 7 475-T 7 351 Alloy Machined with WEDM Process Using The Grey-Based Taguchi Method. Metalurgija/Metallurgy. 2012;51(1):47-50.